Editors' Suggestion

Non-Abelian statistics in light-scattering processes across interacting Haldane chains

Vladimir Gnezdilov,[1,2] Vladimir Kurnosov,[1] Yurii Pashkevich,[3] Anup Kumar Bera,[4,5] A. T. M. Nazmul Islam,[4] Bella Lake,[4,6] Bodo Lobbenmeier,[2] Dirk Wulferding,[7,2,8] and Peter Lemmens[2,8]

[1]*B. Verkin Institute for Low Temperature Physics and Engineering, NASU, 61103 Kharkiv, Ukraine*
[2]*Institute for Condensed Matter Physics, TU Braunschweig, D-38106 Braunschweig, Germany*
[3]*O.O. Galkin Donetsk Institute for Physics and Engineering, NASU, Kyiv - Kharkiv 03028, Ukraine*
[4]*Helmholtz-Zentrum Berlin für Materialien und Energie, 14109 Berlin, Germany*
[5]*Solid State Physics Division, Bhabha Atomic Research Centre, Mumbai 400085, India*
[6]*Institut für Festkörperphysik, Technische Universität Berlin, Hardenbergstr. 36, 10623 Berlin, Germany*
[7]*CCES, Institute for Basic Science, Department Physics and Astronomy, Seoul National University, Seoul 08826, Republic of Korea*
[8]*Laboratory of Emerging Nanometrology LENA, D-38106 Braunschweig, Germany*

(Received 20 June 2021; revised 7 September 2021; accepted 20 September 2021; published 11 October 2021)

The $S = 1$ Haldane state is constructed from a product of local singlet dimers in the bulk and topological states at the edges of a chain. It is a fundamental representative of topological quantum matter. Its well-known archetype, the quasi-one-dimensional $SrNi_2V_2O_8$ shows both conventional as well as unconventional magnetic Raman scattering. The former is observed as one- and two-triplet excitations with small linewidths and energies corresponding to the Haldane gap Δ_H and the exchange coupling J_c along the chain, respectively. Well-defined magnetic quasiparticles are assumed to be stabilized by interchain interactions and uniaxial single-ion anisotropy. Unconventional scattering exists as broad continua of scattering with an intensity $I(T)$ that shows fermionic statistics. Such statistics has also been observed in Kitaev spin liquids and could point to a non-Abelian symmetry. As the ground state in the bulk of $SrNi_2V_2O_8$ is topologically trivial, we suggest its fractionalization to be due to light-induced interchain exchange processes. These processes are supposed to be enhanced due to a proximity to an Ising ordered state with a quantum critical point. A comparison with $SrCo_2V_2O_8$, the $S = 1/2$ analog to our title compound, supports these statements.

DOI: 10.1103/PhysRevB.104.165118

I. INTRODUCTION

Topological effects in condensed matter physics are an attractive field of study as they combine very interesting concepts of fundamental physics with exotic effects, such as anomalous transport in magnetic fields, nonlocal interactions, and fractionalization of excitations [1]. Prominent examples include relativistic Dirac electrons, quantum spin liquids, and the fractional quantum Hall effect.

One of the fundamental aspects of topological systems is that the exchange or braiding of quasiparticles in certain classes of systems leads to an unconventional phase, different from 0 or π, known from bosons and fermions. The resulting non-Abelian statistics has first been realized for the fractional Hall effect at 5/2 filling [2,3]. A planar system with a dimensionality $D < 3$ has to be chosen. Furthermore, weakly interacting quasiparticles should exist that are degenerate in energy for large distances. This leads to the emergent quality of non-Abelian systems.

Periodically driving a system by an electric field is another approach to generate topological states [4–7]. The so-called Floquet Hamiltonian leads to energetically shifted replicas of electron-photon states. Here, the question appears of whether the response to a Laser field may simultaneously induce a non-Abelian statistics by the exchange of quasiparticles [8–10]. Recently, it has been shown that such driving may enhance correlations [11,12] and transfer chain systems from Luttinger liquids to charge density wave instabilities [13]. In principle, light-induced exchange processes between spins S_i and S_j are well known from insulating spin systems and described by the Loudon-Fleury Hamiltonian $\mathcal{H}_{\mathrm{LF}} \sim \sum_{<i,j>} (\mathbf{e}_{\mathrm{in}} \cdot \mathbf{r}_{ij})(\mathbf{e}_{\mathrm{out}} \cdot \mathbf{r}_{ij})\mathbf{S}_i \cdot \mathbf{S}_j$ [14]. Here, the vector $\mathbf{r}_{ij}$ connects spins at sites i and j, and incoming and outgoing light polarizations are denoted by $\mathbf{e}_{\mathrm{in}}$ and $\mathbf{e}_{\mathrm{out}}$, respectively. However, to our knowledge, the topological implications of light-induced spin exchange simultaneously with the Raman scattering process have not been addressed so far.

In the following we focus on $SrNi_2V_2O_8$, a rather well-known representative of weakly interacting Haldane spin chains with $S = 1$ states. This system has a singlet ground state with a spin gap in the bulk and topological states at the surface [1]. For photon energies within the range 1.9–2.5 eV no resonance effects are detected in Raman scattering. Therefore, selection rules of conventional Raman scattering should be valid and follow the dominance of one-dimensional (1D) correlations along the spin chains, as described by the Loudon-Fleury Hamiltonian. Consequently, appreciable intensity should only be observed with a light polarization parallel to the chain direction (c axis). Nevertheless, finite interchain interactions and single ion anisotropies lead to

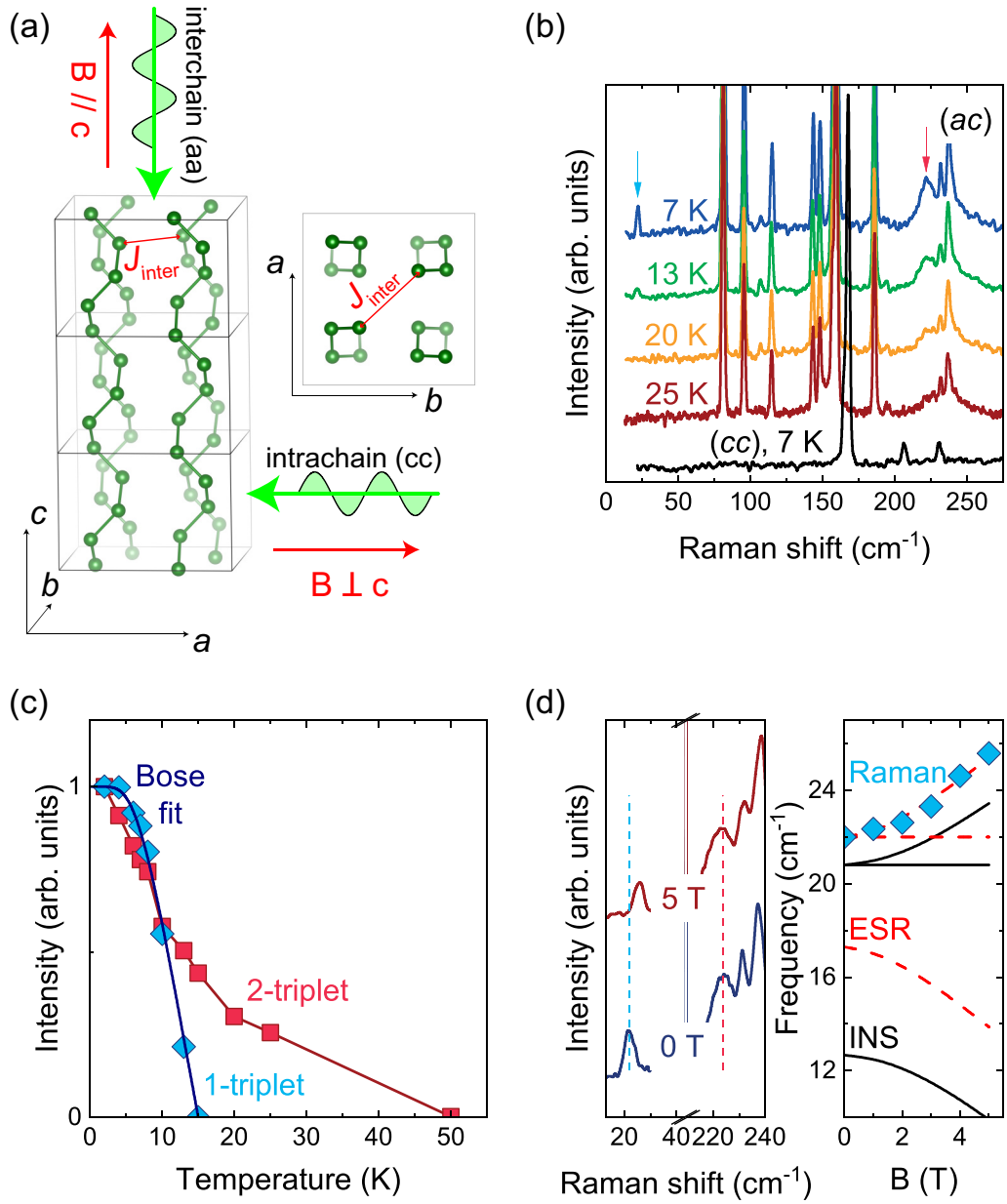

FIG. 1. (a) Four twisted Ni chains along the c axis in two different projections. The scattering geometries are indicated by the green arrows for inter-chain and intra-chain configurations. Red arrows denote the applied magnetic field direction along the chains and perpendicular to the chains. (b) Temperature dependent Raman spectra of $SrNi_2V_2O_8$ obtained in (ac) polarization. The blue and red arrows mark the one- and two-triplet modes, respectively. For comparison, the 7-K spectrum in (cc) polarization is plotted in black. (c) Bose-corrected integrated intensity ($I(T)$) of the magnetic scattering contributions as a function of temperature. The blue line corresponds to a fit using a Bose factor. (d) Effect of a transverse magnetic field on the assigned one- and two-triplet modes. Zero field positions are marked by dashed lines. Transverse magnetic field effect on inelastic neutron scattering (full line), electron spin resonance (ESR) (dashed line) [17–20] and our one-triplet Raman mode (diamonds).

Ising fluctuations and magnetic field induced long range order. With our work we follow the concept of inducing a topological state of an interacting chain system using the Raman scattering process and probe for possible non-Abelian statistics by the measurement process itself. A deconfinement of spinon and holon excitations with non-Abelian statistics has been proposed to exist for $S = 1$ antiferromagnetic systems [15].

In $SrNi_2V_2O_8$ skewed spin chains are formed by edge-sharing NiO_6 (Ni^{2+}, $S = 1$) octahedra along the c axis; see Fig. 1(a). They are coordinated by VO_4^{3-} (V^{5+}, $S = 0$) tetrahedra that weakly hybridize with the Ni-O coordinations. There are four chains per unit cell [16].

All important model parameters are well known [16–22] and the magnetic properties can be summarized as follows: (i) a Haldane gap of $\Delta = 3.6$ meV (29 cm^{-1}) at the AFM zone center ($k = q_{\text{chain}} = \pi$) separates the singlet, spin-liquid ground state from excited triplet states. The relation of the gap and the exchange coupling along the chain gives $\Delta_0 = 0.41J = 0.41 \times 8.7$ meV $= 3.57$ meV (28.6 cm^{-1}).

From ESR two gaps are derived, $\Delta_\perp = 20.8\ \mathrm{cm}^{-1}$ and $\Delta_\parallel = 12.7\ \mathrm{cm}^{-1}$, with a splitting induced by anisotropy. (ii) The triplet excitations show a dispersion up to a maximum energy of $\sim 2.4J$ ($\sim 6.7\Delta$) at the zone boundary ($q_{\mathrm{chain}} = \pi/2$ and $3\pi/2$). (iii) Interchain interactions and anisotropies are given by $J_{\mathrm{inter}} \approx 0.26$ meV and $D = -0.29$ meV [19]. (iv) At the AF zone center the resulting splitted branches are at 1.56 $\pm$ 0.1 meV (12.64 $\pm$ 0.81 cm^{-1}) and 2.58 $\pm$ 0.1 meV (20.90 $\pm$ 0.81 cm^{-1}), respectively [17–19].

II. EXPERIMENTAL DETAILS

Experimental details of the $SrNi_2V_2O_8$ single crystal growth and characterization have been reported earlier [18]. Raman scattering experiments were performed in a quasi-backscattering geometry on *ab* and *ac* surfaces with the excitation wavelength $\lambda = 532.1$ nm and a power level $P =$ 5 mW focused onto a 100-μm-sized spot in parallel [(*aa*), (*cc*)], crossed [(*ab*), (*ac*)], and circular [(*LR*), (*LL*)] light polarizations. Single crystal orientation has been independently assured using the anisotropy of phonon Raman scattering and Laue diffraction method. Raman spectra were measured in a variable temperature closed cycle cryostat and a 10-T superconducting split-coil magnet with the magnetic field along the *c* axis of the crystal.

III. RESULTS AND DISCUSSION

Polarized Raman spectra of $SrNi_2V_2O_8$ show all expected phonon modes and their small linewidth and well-defined selection rules indicate the high sample quality. There are no significant phonon anomalies that would indicate a structural instability [23].

At low temperatures ($T < 30$ K) and in (*ac*) scattering geometry we notice two modes, at 22 cm^{-1} (blue arrow) and at 220 cm^{-1} (red arrow); see Fig. 1(b) and a summary in Table I. The (*ac*) component with one polarization component along the chain direction corresponds to *E* symmetry. The first mode has a rather narrow linewidth and its intensity $I(T)$ is critically depressed with increasing temperatures; see Fig. 1(c), blue symbols. Also an applied transverse magnetic field leads to a characteristic shift; see Fig. 1(d). This shift corresponds very well to previous neutron scattering and ESR data [17–20] of triplet excitations in magnetic fields. Therefore we assign this mode to a one-triplet excitation.

The second mode has a factor 6 larger linewidth. It does not show a pronounced frequency shift with temperature and $I(T)$ is only fully depleted for temperatures above $\sim$30 K, i.e., it is less sensitive to thermal fluctuations. The mode's energy is larger than the maximum energy of the neutron triplet dispersion ($\sim$23 meV, 185 cm^{-1}) [18]. Nevertheless, it fits well to $3J = 210\ \mathrm{cm}^{-1}$.

A similar mode at $3J$ has also been observed in the Haldane chain compound Y_2BaNiO_5 [24]. The factor 3 can be rationalized in an Ising-like spin system considering breaking spin bonds by a spin exchange process. This scheme leads to a typical energy $E_{\mathrm{max}} = (z2S-1)J$ [25,26]. With $S = 1$ and the coordination number, $z = 2$, $E_{\mathrm{max}} = 3J$ is derived. The good agreement of such a heuristic picture of an Ising-like, Néel ground state to an excitation in a quantum disordered system is far from trivial. In 1D or 2D spin liquids a considerable renormalization to lower energies and increasing linewidth is observed [27]. This could imply well-defined quasiparticles and weak fluctuation corrections in this Haldane system. However, it might also mean that these excitations are stabilized by some other mechanism, as discussed later.

We use $I(T) \propto (1 - e^{\Delta/k_BT})$, with singlet-triplet gap $\Delta =$ 3.6 meV, to fit the one-triplet intensity (blue symbols); see solid curve in Fig. 1(c). This fit corresponds to a depression of the Bose-corrected intensity $I(T)$ due to scattering on thermally populated triplets across this gap, i.e., a bosonic statistics. Such a model works very well for $SrCu_2(BO_3)_2$ with orthogonal spin dimers and strongly localized excited triplets [28].

The two-triplet scattering involves double exchange processes averaging over a regime of *k* space around the zone boundary. Therefore a simple analytic expression of $I(T)$ does not exist [26]. The observed smoother dependence is rationalized by a superposition of scattering processes with a dispersing singlet-triplet gap. A second scenario that is relevant for low-dimensional systems considers the importance of local spin-spin correlations. Therefore thermally induced triplet states do not scatter efficiently [27,28].

An unconventional Raman signal is observed between 100 and 280 cm^{-1} with broad maxima and a linewidth of $\approx$200 cm^{-1}. Its onset energy is around 60 cm^{-1} and a high energy cutoff exists at $\approx$350 cm^{-1}; see Fig. 2(a). This signal is only observed in (*LL*) and (*aa*) polarization and not in (*LR*), (*ab*), and (*ac*). Such a strict selection rule points to an intrinsic origin and is not compatible with fluorescence or phonon density of states. Therefore we attribute the continuum to some sort of magnetic/electronic scattering. Interestingly, several phonons appear with asymmetric Fano line shapes on top of this scattering continuum, indicating a resonance between these modes and the continuum. The anomalous temperature dependence of this coupling is detailed in the Appendix.

After subtracting spectral contributions due to phonons (see the Appendix for details) we fit the remaining Bose-corrected spectral weight to a sum of Gaussians, which can approximate the broad, structured continuum. We can identify three major contributions, i.e., lower and higher energy maxima ($C1$, $C2$) and quasielastic scattering (QES). The respective integrated intensities and their sum are given in Fig. 2(b). While $C1$ can be considered as nearly temperature independent, the contribution $C2$ at higher energies exhibits a strong decrease in intensity as the temperature is raised. At lowest temperatures, comparable to the Haldane gap ($\Delta \approx$ 42 K), there is a general drop of intensity. Furthermore, a magnetic field leads to a suppression of the scattering intensity; see the Appendix. For larger magnetic fields $SrNi_2V_2O_8$ shows a quantum phase transition into a Néel-ordered phase.

We notice the very gradual temperature dependence of these intensities, which is in sharp contrast to $I(T)$ of one-triplet and two-triplet scattering [Fig. 1(c)]. However, Raman scattering on quantum spin liquids based on the Heisenberg kagome [29] and the Kitaev honeycomb lattice [30,33] shows a very similar weak temperature dependence. The latter is attributed to their inherent entanglement that make thermal fluctuations ineffective.

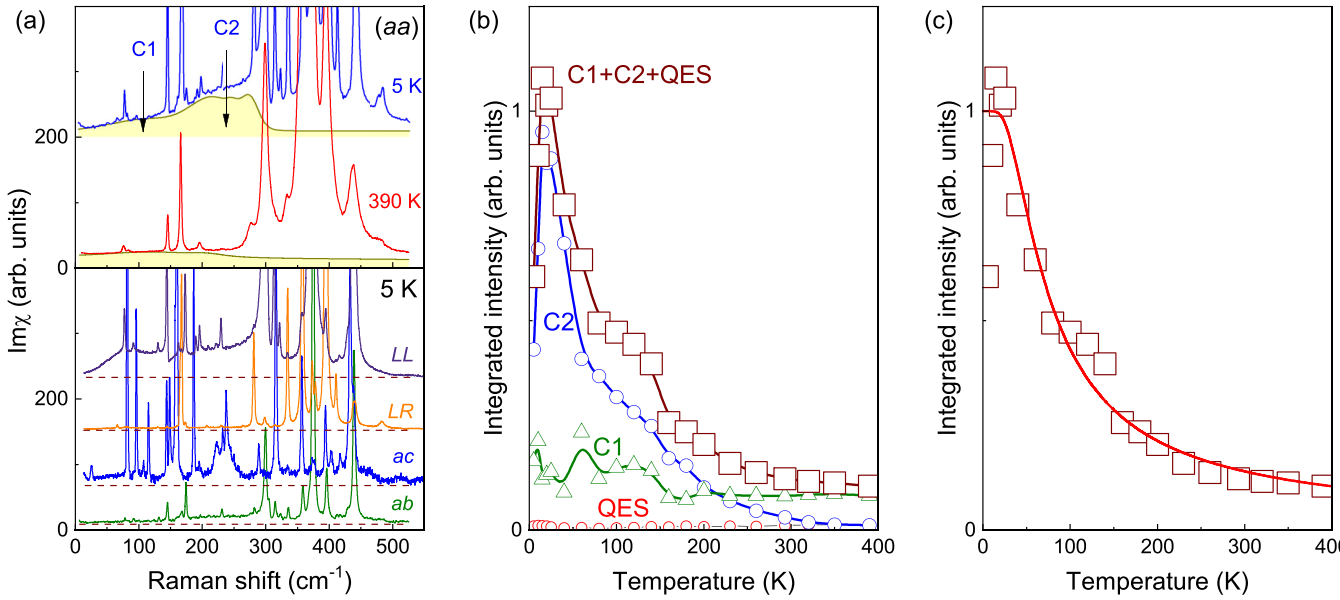

FIG. 2. (a) Bose-corrected Raman spectra of $SrNi_2V_2O_8$ taken perpendicular to the Haldane chain direction in (*aa*) scattering geometry at 7 and 390 K together with low-temperature spectra in (*LL*), (*LR*), and (*ab*) polarization. The yellow-shaded backgrounds represent the unconventional scattering continuum with two maxima, $C1$ and $C2$. (b) Bose-corrected integrated intensities of the $C1$, $C2$, quasielastic scattering (QES, $E \approx 0$), and their sum. The lines are guides to the eye. (c) Fermionic statistics (solid red line) fitted to the summed intensities from (b) (squares)

Also the observation of this mode in (*aa*) polarization with a high energy cutoff is rather unexpected. This polarization has no component along the chain direction with large exchange coupling. The Loudon-Fleury approach implies that the spatial correlations of the exchange integral are probed by the selected light polarization vectors. Due to the small interchain coupling two-particle scattering probed in polarizations perpendicular to the chains should have an energy scale of only $2\Delta_\perp \approx 40\ \mathrm{cm}^{-1}$. On the other hand $SrNi_2V_2O_8$ is rather close to a phase boundary to Ising order due to anisotropy and interchain interaction. Strong fluctuations at such a boundary could favor a more complex mechanism of light scattering beyond the basic Loudon-Fleury approach.

Therefore, we propose an alternative, Floquet-like scenario that consists of a two step process: In a first step, the incident light drives the system into an excited state where spins between neighboring chains are exchanged [e.g., along J_{inter}; see Fig. 1(a)]. These states consist of defects within the topological string order. In the second step these states relax along the chain leading to a high energy scale, comparable to the energy of dispersing triplets. This scenario introduces "edge" states within the topologically protected bulk due to the light-induced spin exchange. The first step can also be replaced by a thermally induced spin flip. This could be the origin of the spectral weight shift in the light-scattering process at elevated temperatures [31]. Such a complex exchange-induced, topological Raman process may also lead to a temperature dependence different from the expected Bose statistics.

The temperature dependence of the continuum, plotted in Fig. 2(c), with its very gradual temperature dependence is completely different from conventional magnetic Raman scattering (as discussed below). Motivated by this difference and the above discussed Raman scattering process we have modeled $I(T)$ by a two-Fermion contribution. This corresponds to an approach used for fractionalized modes in spin liquid states of Kitaev systems [32]. It takes into account that spin liquids carry topological defects due to the creation/annihilation of pairs of fermions (Majorana fermions). Any conventional, bosonic contribution can be neglected after Bose-correcting the Raman scattering intensity. For the Kitaev spin liquid materials α-$RuCl_3$ and different phases of Li_2IrO_3 such a modeling leads to a remarkable description of $I(T)$ [32–37].

In detail, the data are described by a two-Fermion $[1 - f(\omega_F)]^2$ contribution, with $\omega_F = 9.7 \pm 0.9$ meV; see the solid red line in Fig. 2(c). The characteristic energy ω_F is of the or-

TABLE I. Summary of the observed magnetic excitations including energy at the maximum of scattering intensity, polarization, linewidth (Γ). In addition we give the polarization of quasielastic scattering.

Nr	E_{max} (cm^{-1})	Γ (cm^{-1})	Polarization	Parameters	Assignment, comments
1	22	2.5	(*ac*)	$\Delta = 3.6$ meV (29 cm^{-1})	1-triplet, B-dep.
2	220	15	(*ac*)	$E_{\mathrm{max}} \approx 3J$	2-triplet, no B-dep.
3	100–280	≈200	(**aa**, *LL*)	$0{-}6J$, $\omega_F = 9.7$ meV	unconventional continuum
4	≈0		(*aa*)		quasielastic

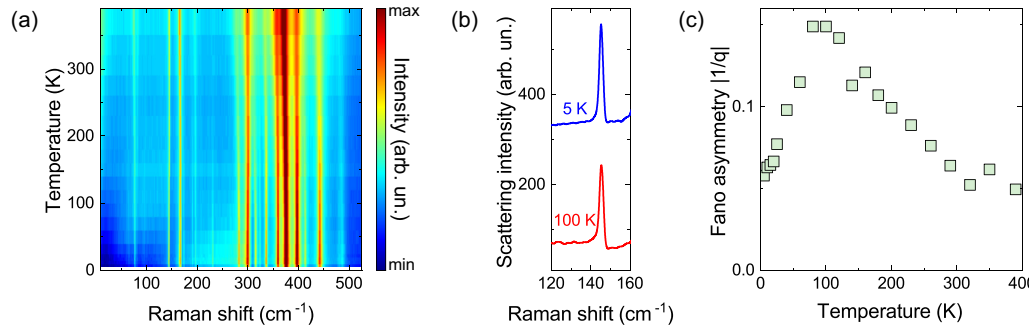

FIG. 3. (a) Color-contour plot of as-measured Raman data in (*aa*) polarization across a temperature range 5–390 K. (b) An asymmetric Fano line shape observed for the 145-cm^{-1} phonon. (c) Temperature dependence of its Fano asymmetry parameter $|1/q|$.

der of the doubled Haldane gap of $SrNi_2V_2O_8$ ($\Delta = 3.6$ meV) giving evidence for an intrinsic origin. The order of magnitude is also comparable to the ones of spin liquid materials mentioned in the previous paragraph.

If we want to rationalize this description it should be noted that the bulk of the Haldane phase is based on a very local product state with a gap and no long range entanglement. In contrast to defects and edges, the bulk does not support fractionalized excitations or edge modes with fermionic statistics. As we have no evidence for defects from magnetic susceptibility data we propose that the measurement process itself (exchange light scattering) and finite temperatures dynamically induce the defects and resulting states. This scenario is reminiscent of the concept of excited state quantum phase transitions [12]. The extracted energy scale ω_F strongly supports this assumption. Furthermore, the high cutoff energy E_{cutoff} and the large linewidth of the order of 5–6J are not compatible with the coordination number $z = 2$ of a 1D chain.

Within the scheme of exchange-induced, broken bonds a maximum at about 3J would be expected, in excellent agreement with the observed broad maxima. The strict selection rules of the continuum with all components perpendicular to the chain evidence that the existing correlations are rather two dimensional contrasting the dominating chain exchange that exists in the ground state. On the other side, recent Floquet modeling of periodically driven Mott insulators show nonequilibrium steady states with an enhancement of correlations [11].

Finally, we note that our Raman experiments on the isostructural $S = 1/2$ analog $SrCo_2V_2O_8$ shows an in-chain, spinon continuum in good agreement with neutron scattering data [38]. There is no evidence for high energy scattering with out-of-chain polarizations. The corresponding data are shown in the Appendix.

We summarize the properties of all three modes attributed to magnetic Raman scattering in Table I. They clearly differ with respect to energy, linewidth, polarization, and in their dependence on temperature, as well as on an external magnetic field.

IV. SUMMARY

The presented polarization-resolved Raman spectra of single crystalline $SrNi_2V_2O_8$ provide a view of the manifold of excited states in a quasi-one-dimensional $S = 1$ Haldane system close to a critical state. Besides a one-triplet and a two-triplet mode, a broad continuum is observed that we attribute to an exited state Raman process induced by the exchange process itself. The proposed scattering mechanism involves the generation of a light-induced topological interchain defect that relaxes via a high energy, intrachain process. We have discussed the high cutoff energy of this process to be related to enhanced dimensionality (2D) or a Floquet-like enhancement of electronic correlations.

ACKNOWLEDGMENTS

We acknowledge important discussions with W. Brenig, J. Knolle, and S. R. Manmana. This research was funded by the Deutsche Forschungsgemeinschaft Excellence Cluster QuantumFrontiers, EXC 2123 - 390837967, as well as by Deutsche Forschungsgemeinschaft (DFG) Le967/16-1, Deutsche Forschungsgemeinschaft DFG-RTG 1952/1, and the Quantum- and Nano-Metrology (QUANOMET) initiative within project NL-4. D.W. acknowledges support by the Institute for Basic Science (Grant No. IBS-R009-Y3). B.L. acknowledges the support of the Deutsche Forschungsgemeinschaft (DFG) through the project B06 of the SFB-1143 (ID247310070).

APPENDIX

To shed a light on possible lattice instabilities and phonon anomalies, we show the as-measured Raman scattering intensity in (*aa*) polarization as a color-contour plot in Fig. 3(a). All observed phonons show a rather static temperature evolution, without any evidence for a structural phase transition. A closer look reveals, however, that phonon anomalies exist in the form of Fano asymmetries that describe a coupling of a discrete mode (phonon) to an extended continuum of states. This effect is especially pronounced for an in-plane phonon of B_1 symmetry located around 145 cm^{-1} [23] [see Fig. 3(b)], which suggests its coupling to the underlying continuum of spin excitations. Its Fano asymmetry shows a clear temperature dependence with a maximum at about 100 K and a drop to lower temperatures, shown in Fig. 3(c). This dependence resembles to some extent that of the continuum's intensity in Fig. 2(c). On the other hand, the energy of the continuum itself displays a strong temperature dependence [see Fig. 2(a)]: at 5 K its spectral weight is mostly located at $E > 145$ cm^{-1}, while at 390 K it has shifted to $E < 145$ cm^{-1}. Therefore, the

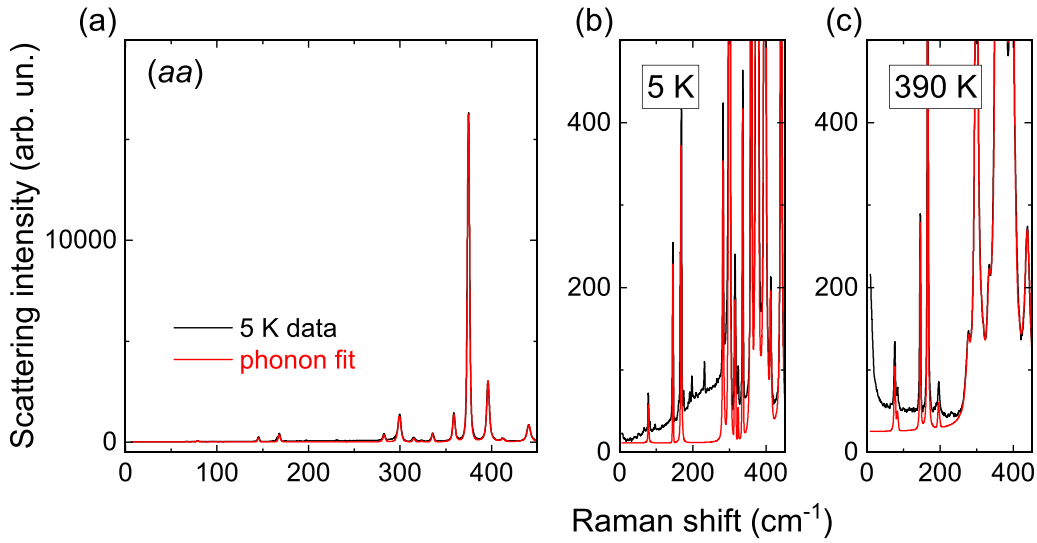

FIG. 4. (a) Raman spectrum obtained at $T = 5$ K (black curve) together with a fit of the phonons (red line). (b) Zoom-in at small intensities. (c) Comparison between $T = 390$ K data and phonon fit.

temperature dependence of the Fano asymmetry mainly reflects the temperature-dependent redistribution of the spectral weight. Phonon frequencies, on the other hand, do not show any distinct temperature anomalies. Spin-phonon coupling of conventional materials in mean field approximation relies on a coupling of the magnetization density or energy density

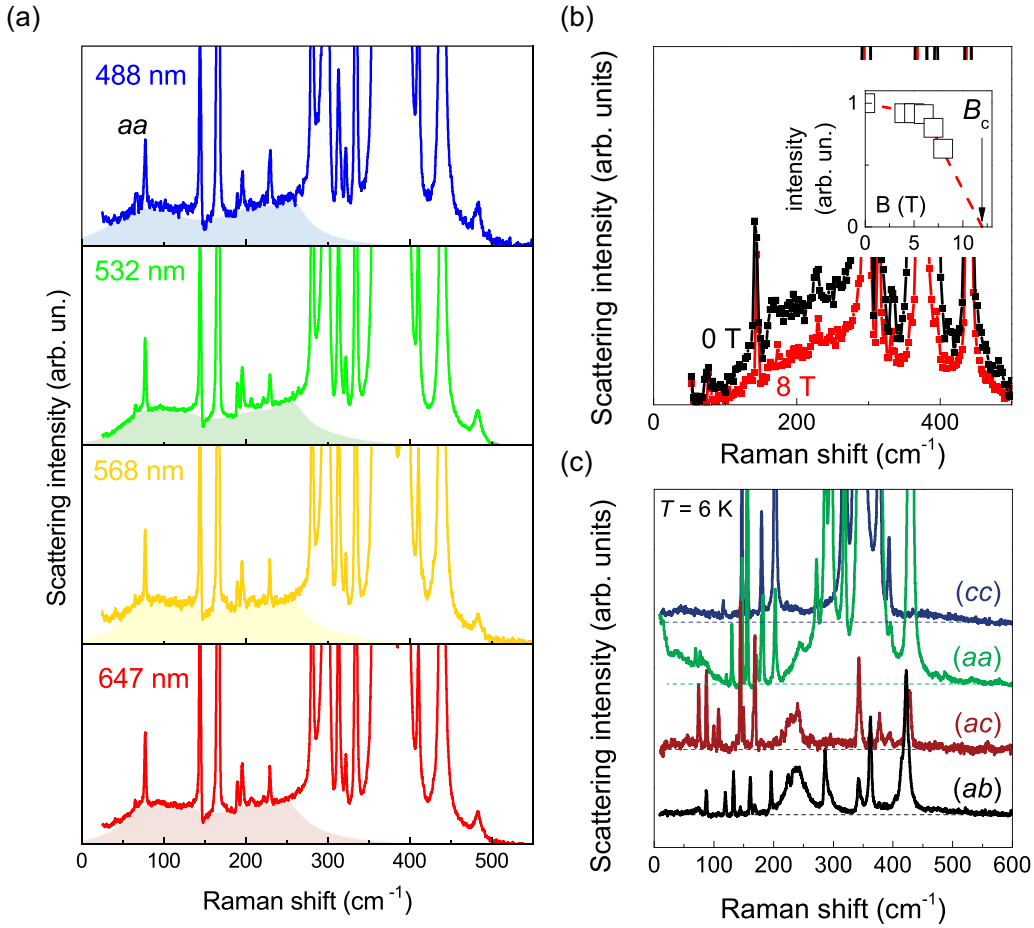

FIG. 5. (a) Raman data obtained at $T = 6$ K and in (*aa*) polarization using various laser energies. (b) Magnetic field (B) dependence of the scattering continuum in (*ab*) polarization. The inset plots its integrated intensity over B. (c) Polarization-resolved Raman data of the isostructural $S = 1/2$ system $SrCo_2V_2O_8$.

(as function of temperature). Pronounced effects therefore assume large changes at characteristic temperature (e.g., at T_N) due to critical fluctuations. In the present Haldane system, the number of thermally induced triplet states is too small and only gradually increasing with temperature.

A detailed analysis of the Raman spectrum measured in (aa) polarization at 5 K is shown in Fig. 4(a). The complete fit (red curve) consists of a number of Lorentzian line shapes and it captures the overall phonon spectrum well. A zoom-in at small intensities [Fig. 4(b)] reveals that a broad background remains. As the linewidths of the phonons are significantly smaller compared to the broad continuum, both contributions can be well separated. Although the overlap around 300–400 cm^{-1} still obscures some details of the continuum, we can be rather confident about its spectral shape up to 300 cm^{-1}. Figure 4(c) compares the Raman data and the phonon fit at $T = 390$ K.

Next we investigate whether resonance effects or the skewed spin chains formed by edge-sharing NiO_6 octahedra along the c axis are responsible for the broad continua of magnetic/electronic Raman scattering. Therefore we did detailed investigations using lasers of different photon energies. Furthermore, we studied the related, Co based $SrCo_2V_2O_8$ system with similar local coordinations and comparable intrinsic energy scales. In Fig. 5(a) four data sets are given with the indicated wavelength of the incident laser radiation. The general shape and spectral weight continuum does not evidence any effect. This supports our assumption that it is of intrinsic origin and not related to other (e.g., fluorescence) processes. We also note that the continuum's intensity shows no significant laser energy dependence. In Fig. 5(b) the intensity of the continuum as a function of magnetic field is plotted. Here the magnetic field is aligned along the crystallographic c axis, parallel to the chain direction. Since the mode is sensitive to external magnetic fields, we can assume that it is of magnetic origin. Furthermore, its intensity is strongly decreased for fields approaching 12 T, which corresponds to the critical field. At larger fields, full spin polarization is achieved [19].

In the isostructural sister compound $SrCo_2V_2O_8$ we find no evidence for a comparable broad continuum with a polarization perpendicular to the chain direction [see Fig. 5(c)]. $SrCo_2V_2O_8$ is the $S = 1/2$ analog to our title compound. Hence, its excitation spectrum is gapless and no topology-related edge states exist, in accordance with our data. Taken together, these observations strongly support our interpretation of the broad signal emerging in Raman scattering experiments on $SrNi_2V_2O_8$.

[1] F. D. M. Haldane, Phys. Rev. Lett. **50**, 1153 (1983); Phys. Lett. A **93**, 464 (1983); Rev. Mod. Phys. **89**, 040502 (2017).
[2] X. G. Wen, Phys. Rev. Lett. **66**, 802 (1991).
[3] G. Moore and N. Read, Nucl. Phys. B **360**, 362 (1991).
[4] V. Khemani, A. Lazarides, R. Moessner, and S. L. Sondhi, Phys. Rev. Lett. **116**, 250401 (2016).
[5] T. Morimoto and N. Nagaosa, Sci. Adv. **2**, e1501524 (2016).
[6] Y. H. Wang, H. Steinberg, P. Jarillo-Herrero, and N. Gedik, Science **342**, 453 (2013).
[7] I. Esin, M. S. Rudner, G. Refael, and N. H. Lindner, Phys. Rev. B **97**, 245401 (2018).
[8] J. E. Moore, Physics **2**, 82 (2009).
[9] W. Bishara, P. Bonderson, C. Nayak, K. Shtengel, and J. K. Slingerland, Phys. Rev. B **80**, 155303 (2009).
[10] M. Vogl, M. Rodriguez-Vega, and G. A. Fiete, Phys. Rev. B **101**, 024303 (2020).
[11] F. Peronaci, O. Parcollet, and M. Schiró, Phys. Rev. B **101**, 161101(R) (2020).
[12] P. Cejnar, P. Stránský, M. Macek, and M. Kloc, J. Phys. A: Math. Theor. **54**, 133001 (2021).
[13] D. M. Kennes, A. de la Torre, A. Ron, D. Hsieh, and A. J. Millis, Phys. Rev. Lett. **120**, 127601 (2018).
[14] P. A. Fleury and R. Loudon, Phys. Rev. **166**, 514 (1968).
[15] M. Greiter and R. Thomale, Phys. Rev. Lett. **102**, 207203 (2009).
[16] A. K. Bera and S. M. Yusuf, Phys. Rev. B **86**, 024408 (2012).
[17] A. K. Bera, B. Lake, A. T. M. N. Islam, B. Klemke, E. Faulhaber, and J. M. Law, Phys. Rev. B **87**, 224423 (2013).
[18] A. K. Bera, B. Lake, A. T. M. N. Islam, O. Janson, H. Rosner, A. Schneidewind, J. T. Park, E. Wheeler, and S. Zander, Phys. Rev. B **91**, 144414 (2015).
[19] A. K. Bera, B. Lake, A. T. M. N. Islam, and A. Schneidewind, Phys. Rev. B **92**, 060412(R) (2015).
[20] Z. Wang, M. Schmidt, A. K. Bera, A. T. M. N. Islam, B. Lake, A. Loidl, and J. Deisenhofer, Phys. Rev. B **87**, 104405 (2013).
[21] B. Pahari, K. Ghoshray, R. Sarkar, B. Bandyopadhyay, and A. Ghoshray, Phys. Rev. B **73**, 012407 (2006).
[22] Z. He and Y. Ueda, J. Phys. Soc. Jpn. **77**, 013703 (2008).
[23] V. Kurnosov, V. Gnezdilov, P. Lemmens, Yu. Pashkevich, A. K. Bera, A. T. M. N. Islam, and B. Lake, Low Temp. Phys. **43**, 1405 (2017).
[24] P. E. Sulewski and S.-W. Cheong, Phys. Rev. B **51**, 3021 (1995).
[25] W. Hayes and R. Loudon, *Scattering of Light by Crystals* (John Wiley & Sons, New York, 1978).
[26] M. G. Cottam and D. J. Lockwood, *Light Scattering in Magnetic Solids* (John Wiley & Sons, New York, 1986).
[27] P. Lemmens, G. Güntherodt, and C. Gros, Phys. Rep. **375**, 1 (2003).
[28] P. Lemmens, M. Grove, M. Fischer, G. Güntherodt, V. N. Kotov, H. Kageyama, K. Onizuka, and Y. Ueda, Phys. Rev. Lett. **85**, 2605 (2000).
[29] D. Wulferding, P. Lemmens, P. Scheib, J. Röder, P. Mendels, S. Chu, T. Han, and Y. S. Lee, Phys. Rev. B **82**, 144412 (2010).
[30] A. Glamazda, P. Lemmens, S.-H. Do, Y. S. Choi, and K.-Y. Choi, Nat. Commun. **7**, 12286 (2016).
[31] J. Becker, T. Köhler, A. C. Tiegel, S. R. Manmana, S. Wessel, and A. Honecker, Phys. Rev. B **96**, 060403(R) (2017).
[32] J. Nasu, J. Knolle, D. L. Kovrizhin, Y. Motome, and R. Moessner, Nat. Phys. **12**, 912 (2016).
[33] L. J. Sandilands, Y. Tian, K. W. Plumb, Y.-J. Kim, and K. S. Burch, Phys. Rev. Lett. **114**, 147201 (2015).
[34] J. Knolle, D. L. Kovrizhin, J. T. Chalker, and R. Moessner, Phys. Rev. Lett. **112**, 207203 (2014).
[35] J. Knolle, G.-W. Chern, D. L. Kovrizhin, R. Moessner, and N. B. Perkins, Phys. Rev. Lett. **113**, 187201 (2014).

[36] B. Perreault, J. Knolle, N. B. Perkins, and F. J. Burnell, Phys. Rev. B **92**, 094439 (2015).

[37] J. Nasu, M. Udagawa, and Y. Motome, Phys. Rev. Lett. **113**, 197205 (2014).

[38] A. K. Bera, B. Lake, F. H. L. Essler, L. Vanderstraeten, C. Hubig, U. Schollwöck, A. T. M. N. Islam, A. Schneidewind, and D. L. Quintero-Castro, Phys. Rev. B **96**, 054423 (2017).